Measurement Science and Technology

100 year anniversary
Measurement Science and Technology

PAPER

A self-calibrating multicomponent force/torque measuring system

IOP Publishing Measurement Science and Technology
Meas. Sci. Technol. **29** (2018) 074002 (9pp) https://doi.org/10.1088/1361-6501/aac00f

A self-calibrating multicomponent force/ torque measuring system

Rafael R Marangoni[1], Jan Schleichert[1], Ilko Rahneberg[2], Falko Hilbrunner[3] and Thomas Fröhlich[1]

[1] Institute for Process Measurement and Sensor Technology, Ilmenau University of Technology, 98693 Ilmenau, Germany
[2] SIOS Meßtechnik GmbH, Research & Development, 98693 Ilmenau, Germany
[3] Sartorius Lab Instruments GmbH & Co. KG, 37075 Göttingen, Germany

E-mail: rafael.marangoni@tu-ilmenau.de

Received 31 January 2018, revised 12 April 2018
Accepted for publication 25 April 2018
Published 17 May 2018

Abstract

A multicomponent self-calibrating force and torque sensor is presented. In this system, the principle of a Kibble balance is adapted for the traceable force and torque measurement in three orthogonal directions. The system has two operating modes: the velocity mode and the force/torque sensing mode. In the velocity mode, the calibration of the sensor is performed, while in the force/torque sensing mode, forces and torques are measured by using the principle of the electromagnetic force compensation. Details about the system are provided, with the main components of the sensor and a description of the operational procedure. A prototype of the system is currently being implemented for measuring forces and torques in a range of ± 2 N and ± 0.1 N $\cdot$ m respectively. A maximal relative expanded measurement uncertainty ($k = 2$) of $1 \cdot 10^{-4}$ is expected for the force and torque measurements.

Keywords: force measurement, torque measurement, multicomponent, traceable measurement, Kibble balance, calibration

(Some figures may appear in colour only in the online journal)

1. Introduction

Several calibration setups for multicomponent force and torque sensors have been presented in the literature. For instance, the Physikalisch-Technische Bundesanstalt (PTB) in Germany has two calibration setups [1, 2] used for calibrating multi-component sensors. The first system can be used to calibrate six component force and torque sensors and has a measuring range of up to 10 kN for the forces and 1 kN$\cdot$ m for the torques. With this system it is possible to measure forces and torques with a relative expanded measurement uncertainty ($k = 2$) of $2.2 \cdot 10^{-4}$. The second system is a deadweight force/torque standard machine and can be used to calibrate two-component systems. It has a range from 20 kN to 1 MN for the force component and 20 N$\cdot$ m to 2 kN$\cdot$ m for the torque component. Using this device forces and torques can be calibrated with expanded relative uncertainties ($k = 2$) of $2 \cdot 10^{-5}$ and $3.9 \cdot 10^{-4}$ respectively. Other works have addressed the calibration of multicomponent force and torque sensors in different measuring ranges. For instance, Ferrero *et al* [3] have developed a six-component system that operates with forces up to 105 kN and torques up to 2 kN$\cdot$ m. Kim *et al* [4] have developed a system that generates forces and torques in ranges of 50 N to 500 N and 5 N$\cdot$ m to 50 N$\cdot$ m respectively. At the NASA Langley Research Center different calibration setups have been designed as well. The single-vector force balance calibration system (SVS) can be used to calibrate six-component sensors and generate forces and torques up to 700 N and 28 N$\cdot$ m respectively [5]. The variable acceleration force calibration system (VACS) can be used to generate forces and torques up to 130 N and 13 N$\cdot$ m respectively [6]. For forces and torques in the range of 0.6 N and 31 mN$\cdot$ m a calibration setup was designed at the Technische Universität Ilmenau [7]. With this system it is possible to generate forces and torques with a relative expanded uncertainty ($k = 2$) of $2.1 \cdot 10^{-4}$ and $4.7 \cdot 10^{-3}$ respectively. Table 1 shows these systems with the respective relative expanded ($k = 2$) measurement uncertainties that can be achieved for both force and torque measurements.

Table 1. Calibration force and torque ranges of multicomponent calibration setups and relative expanded measurement uncertainties ($k = 2$) in brackets.

System[a]	F_x	F_y	F_z	M_x	M_y	M_z
PTB-2 [2]	—	—	1 MN		—	2 kN· m
	—	—	($2.0 \cdot 10^{-5}$)	—	—	($3.9 \cdot 10^{-4}$)
PTB-6 [1]	10 kN	10 kN	10 kN	1 kN· m	1 kN· m	1 kN· m
	($1.6 \cdot 10^{-4}$)	($1.4 \cdot 10^{-4}$)	($1.5 \cdot 10^{-4}$)	($2.0 \cdot 10^{-4}$)	($2.0 \cdot 10^{-4}$)	($1.6 \cdot 10^{-4}$)
INRiM [3]	6 kN	6 kN	105 kN	2 kN· m	2 kN· m	2 kN· m
	($6 \cdot 10^{-4}$)	($6 \cdot 10^{-4}$)	($4 \cdot 10^{-5}$)	($1 \cdot 10^{-3}$)	($1 \cdot 10^{-3}$)	($1 \cdot 10^{-3}$)
GNU [4]	500 N	500 N	500 N	50 N· m	50 N· m	50 N· m
	($8.6 \cdot 10^{-4}$)	($8.6 \cdot 10^{-4}$)	($1.2 \cdot 10^{-5}$)	($8.6 \cdot 10^{-4}$)	($8.6 \cdot 10^{-4}$)	($1.7 \cdot 10^{-3}$)
NASA-SVS [5, 8]	220 N	350 N	700 N	11 N· m	28 N· m	14 N· m
	($2.0 \cdot 10^{-4}$)	($2.0 \cdot 10^{-4}$)	($1.8 \cdot 10^{-4}$)	($1.3 \cdot 10^{-3}$)	($4.6 \cdot 10^{-4}$)	($4.8 \cdot 10^{-4}$)
NASA-VACS [6]	90 N	—	130 N	—	13 N· m	—
	($1.3 \cdot 10^{-2}$)	—	($7.5 \cdot 10^{-3}$)	—	($8.4 \cdot 10^{-3}$)	—
TU-Ilmenau [7]	0.6 N	0.6 N	0.6 N	31 mN· m	31 mN· m	31 mN· m
	($2.1 \cdot 10^{-4}$)	($2.1 \cdot 10^{-4}$)	($2.1 \cdot 10^{-4}$)	($4.7 \cdot 10^{-3}$)	($4.7 \cdot 10^{-3}$)	($4.7 \cdot 10^{-3}$)

[a] The names used in this description refer to the institutions where the systems were developed.

A common fact for all systems mentioned here is that the forces and torques are realized either by deadweights or by calibrated force/torque sensors. For the systems based on deadweights there is an additional difficulty to apply horizontal forces, which are normally generated in the vertical, i.e. gravity acceleration direction. In this case, it is necessary to use additional mechanisms with levers, bearings or pulleys, to conduct the forces, or rotate the force sensor in order to align the direction to be calibrated with the gravity direction. Alternatively, the test forces by the deadweight can be generated by moving the sensor with a known acceleration along the desired direction [6]. It is also possible to overcome these difficulties by using calibrated force/torque sensors as measurement standards, which can operate in any orientation. However, the force and torque sensors are usually calibrated by using deadweight machines and limited by the uncertainties obtained with these calibration systems.

In this paper, a self-calibrating multicomponent force/torque measuring system based on the Kibble balance principle [9, 10] is introduced. Kibble balances are currently being used for the redefinition of the kilogram in the revised International System of Units [11, 12]. The system presented here is a realization of the principle first described in [13] and includes reference standards for position, angle, voltage, resistance and time, which are used to provide traceable measurements for the calibration factors of the sensor. In this way, calibration methods only based on electrical, time, length and angle measurements are necessary. So, the use of deadweights and the gravitational acceleration $\vec{g}$ are avoided. It is possible to use this system as a force and torque measurement standard, to calibrate other sensors, and also to measure forces and torques in different applications, providing a traceable measurement with improved uncertainty through in-process calibration. Furthermore, the system is based on the principle of the electromagnetic force compensation (EMFC), which has been used in high precision balances since more than 70 years [14, 15], and includes the following advantages: there is no displacement of the sensing element during the measuring process and nonlinearities in material deformations are avoided [16, 17]. The system presented here has not only the potential to simplify the traceable measurement of forces and torques, but also to improve the measurement uncertainty in the force/torque range covered by the device. It is designed for measuring forces and torques in a range of ± 2 N and ± 0.1 N· m respectively, including applications in the Lorentz force velocimetry [18, 19], micromachining [20] and biomechatronics [21–24].

2. Description of the system

The main component of the system is a levitating servo controlled element with six position sensors and twelve voice coil actuators attached to it (figure 1). The voice coil actuators are divided in two groups of six actuators each. We name them coils A and coils B in the following. The system has also two operating modes, called the velocity mode and the force/torque sensing mode. By using a multi-input multi-output (MIMO) control system, the signals from the six position sensors and the forces generated by six voice coil actuators, it is possible to control the position and angle of the floating element to any desired level inside the range of motion. In the velocity mode, the coils B are used as actuators and the control system has sine wave reference trajectories for the position and angles. The use of a sine wave as reference trajectory during the velocity mode has already been described in [25–27] for different Kibble balance experiments. While the sensing element moves with the given trajectory, the voltages induced in the coils A are measured. The calibration coefficients for the force and torque measurements can be determined by using the amplitude of the induced voltages and the amplitude of the linear and angular velocities, which were measured during the velocity mode. In the force/torque sensing mode, the coils A are used as actuators and the sensing element is controlled to a constant position and angle. External forces and torques

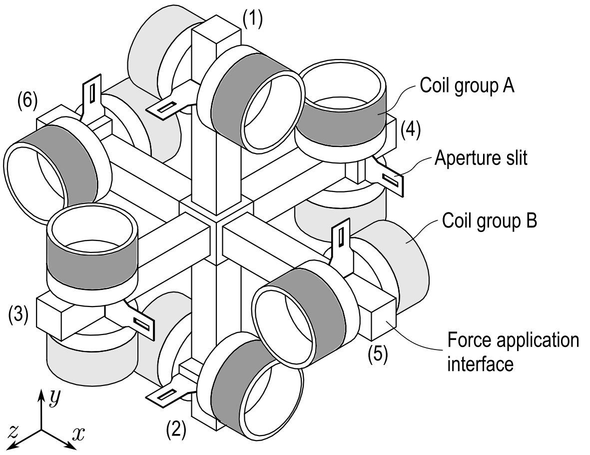

Figure 1. The sensing element with the coils of the actuators and the aperture slits.

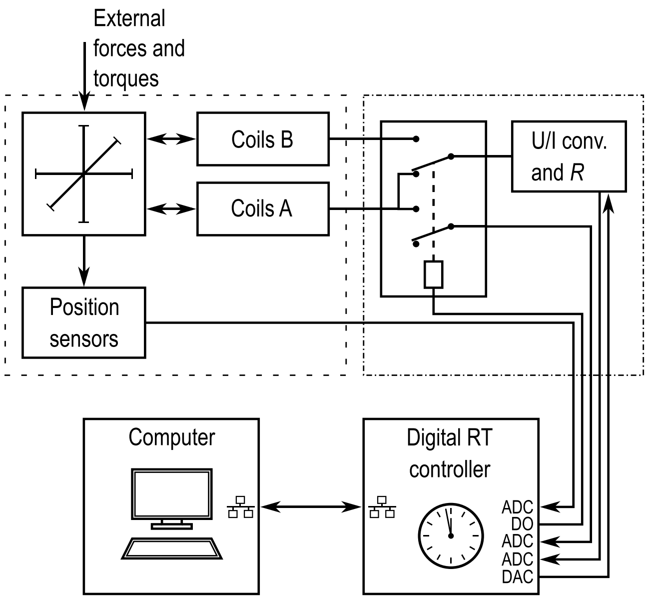

Figure 2. System plan with the main components. The dashed line represents the sensor with the sensing elements and the dash dotted line represents the electronics with U/I converters, measuring resistors and switching system.

acting on the sensing element are compensated by the control system and can be determined by measuring the current flowing in the coils A and using the calibration factors determined in the velocity mode. A six coil system that operates only in the force/torque sensing mode was already described in [17].

The system is designed to measure forces and torques in a range of ± 2 N and $\pm 0{,}1$ N $\cdot$ m respectively with a maximal relative expanded measurement uncertainty ($k = 2$) of $1 \cdot 10^{-4}$. In order to achieve this uncertainty, all components of the system (figure 2) have to fulfill specific requirements of stability and linearity and some of them need to be measured traceable to the SI. This includes the position sensors, the resistance standards, voltage measuring systems and time reference. In the following sections, more details for each component are provided with the respective requirements.

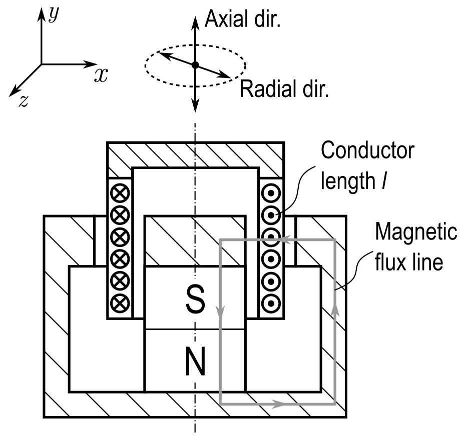

Figure 3. Voice coil actuator with permanent magnet.

2.1. Voice coil actuators

A sketch of the voice coil actuators used in this system is shown in figure 3. They are composed of a NdFeB permanent magnet, a ferromagnetic flux guide and a coil. The magnitude of the static force generated by each voice coil actuator is given by the following expression:

$$F = k_{Bl} i \tag{1}$$

where k_{Bl} indicates the calibration factor of the voice coil actuator, which is proportional to the product of the magnetic flux density B with the length of the conductor l. All voice coil actuators have a nominal value for k_{Bl} equal to 20 N/A. The magnitude of the torque generated by the voice coil actuators is given by:

$$T = k_{dBl} i \tag{2}$$

where k_{dBl} is the calibration factor for the torque, which is proportional to B, l and the distance d between the axis of the coil and the torque center of the sensing element. The torque center is the reference point for the torque measurement and can be virtually fixed to any position. In our case it is defined in the geometric center of the sensing element. All voice coil actuators have a nominal value for k_{dBl} equal to 1 N$\cdot$ m A^{-1}.

As described in [17], there are two voice coil actuators for each measurement direction, responsible for generating the respective force and torque components. For instance, the coils A-1 and A-2 generate the following static force and torque components:

$$F_x = F_1 + F_2 = k_{Bl1} i_1 + k_{Bl2} i_2 \tag{3}$$

$$T_z = T_1 + T_2 = -k_{dBl1} i_1 + k_{dBl2} i_2. \tag{4}$$

These expressions are for the force/torque sensing mode, when the coils A compensate the external forces and torques applied to the sensing element. For the velocity mode the following expressions can be obtained:

$$u_{Bl1} = \hat{k}_{Bl1} v_x \quad \text{and} \quad u_{Bl2} = \hat{k}_{Bl2} v_x \tag{5}$$

$$u_{dBl1} = \hat{k}_{dBl1} \Omega_z \quad \text{and} \quad u_{dBl2} = \hat{k}_{dBl2} \Omega_z \tag{6}$$

u_{Bl1} and u_{Bl2} represent the voltages induced in the coils A-1 and A-2 when the sensing element is moved along the x

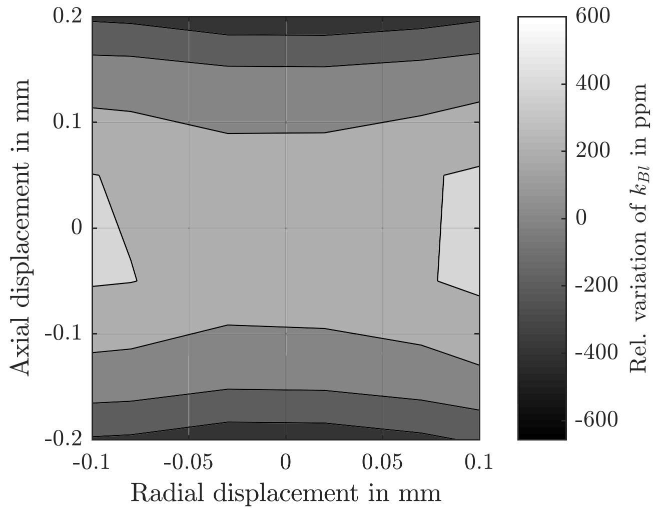

Figure 4. k_{Bl} as a function of the position of the voice coil [29].

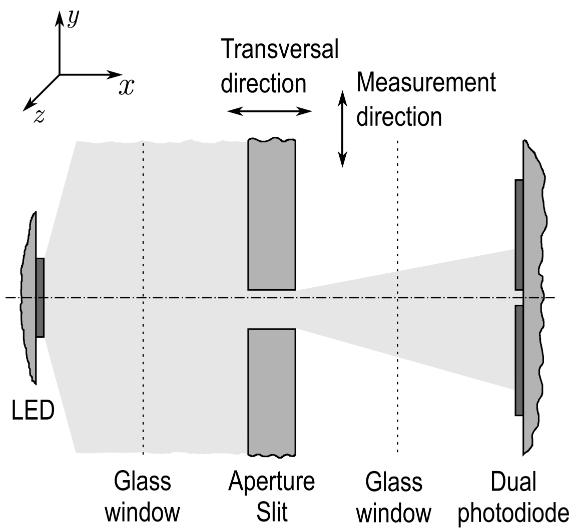

Figure 5. Position sensor with LED, aperture slit and dual photodiode [31].

direction with a velocity amplitude v_x. u_{dBl1} and u_{dBl2} are the voltages induced in the same coils when the sensing element is rotated with angular velocity amplitude Ω_z. This rotation must be about an axis that intersects the torque center and is parallel to the z direction.

As described in [28], velocity components orthogonal to the axis of the coil or in angular directions generate additional induced voltages. These voltages cause an error in the determination of k_{Bl} and have to be considered. In traditional Kibble balance experiments, these effects are minimized by careful alignment of the balance [9, 10]. A different strategy is used in this multicomponent sensor. All linear and angular velocity components are measured and controlled, in a way to generate a precise movement parallel to the coil axis. By doing so, these effects are expected to be negligible.

The working principle of the sensor relies on the fact that $k_{Blj} = \hat{k}_{Blj}$ and $k_{dBlj} = \hat{k}_{dBlj}$, for $j = 1, \ldots, 6$. In this way it is possible to determine the calibration coefficients k_{Blj} and k_{dBlj} of the force and torque sensor during the velocity mode and use them to obtain a traceable force and torque measurement during the force/torque sensing mode. However, there are several assumptions necessary for this principle to work. The magnitude of the magnetic flux generated by the permanent magnets depends on the temperature of the magnetic material. For NdFeB magnets this dependence is about $-0.1\%\ \mathrm{K}^{-1}$ [30]. After determining the calibration coefficients during the velocity mode, the temperature of the permanent magnets must be monitored to avoid error influences originated by temperature variation. It is known that this influence can be minimized by using SmCo magnetic materials, which have a lower temperature coefficient. The calibration factors k_{Blj} and k_{dBlj} of the coils A depend on the relative position and angle of the coil to the permanent magnet. A measurement result that describes this dependence for k_{Blj} is shown in figure 4. The position and angle of the sensing element must be the same for both velocity and force/torque sensing modes, and the amplitude of the movement during the velocity mode must not be too high in order to avoid error effects caused by nonlinearities of the actuators. During the velocity mode, the sensing element has also to precisely follow the moving trajectories. The precise movement is assured by the position sensors, which are discussed in the next section.

In publications about Kibble balances [9] the calibration factor for the electromagnetic actuator is usually given as the direct product of the magnetic flux B by the conductor length l. In these balances the magnet system is designed in a way to produce a magnetic field as uniform as possible in the region occupied by the coil, and the range of motion of the coil during the velocity mode is normally several millimeters. For instance, the coil of the NIST-4 can move more than 40 mm during the velocity mode [10]. This is not the case for the magnet system used in this work, and the magnetic flux density here is not as uniform as in traditional Kibble balances. For this reason, the calibration factor of the electromagnetic actuator is given by k_{Bl}, which corresponds to the integration of a non-uniform magnetic flux density B along the axial direction. Since the range of motion of the coil is much lower here (60 μm) the design requirements of the magnet system are lowered and a non-uniform B can be tolerated.

2.2. Position sensors

The position measuring system used in the force/torque sensor is shown in the figure 5. It is composed by a LED light source, an aperture slit and a dual photodiode. The LED and the dual photodiode are fixed to the sensor frame and the aperture slit is attached to the sensing element. As the aperture slit moves in the measurement direction, the light intensity in each photodiode changes. The currents driven by the photodiodes are proportional to the light intensity. The position of the aperture slit in the measurement direction can be obtained by measuring the currents of both photodiodes and calculating the difference between them:

$$y_{al} = k_{ps}\,(i_u - i_l) \tag{7}$$

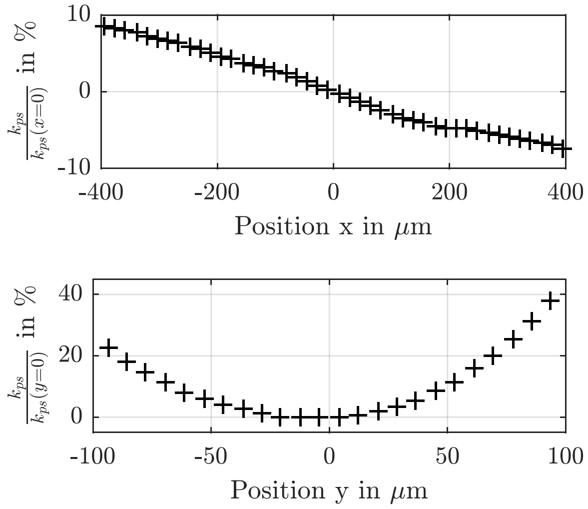

Figure 6. Sensitivity of the position sensor as a function of the displacement in transversal and measurement directions.

where i_u and i_l represent the currents driven by the upper and lower photodiodes respectively and k_{ps} represents the gain of the position sensor. In order to measure the three position coordinates and angles of the sensing element it is necessary to use six of these position sensors.

There are several aspects of these position sensors that must be considered for consistently measuring the position and angles of the sensing element. These position sensors have a nonlinear characteristic curve and the gain k_{ps} depends on the position of the aperture slit relative to the dual photodiode. Figure 6 contains results of measurements performed to quantify these effects. The non-linearity of the characteristic curve is shown by k_{ps} as a function of the position of the aperture slit in y direction, i.e. measurement direction. The gain k_{ps} as a function of the position in the x direction, i.e. transversal direction, is shown in the same figure. There are also several uncertainties introduced due to assembly tolerances of the aperture slits, the LEDs and the photodiodes. In order to achieve the desired relative uncertainty for the force and torque measurement it is necessary to measure the position and angle amplitudes during the velocity mode with relative standard uncertainties smaller than $34 \cdot 10^{-6}$. The strategy used in this case is to calibrate the whole position and angle measuring system, which includes the six individual position sensors, with a triple-beam laser interferometer (figure 7). This laser interferometer can be used to measure a position coordinate and two angles of a mirror attached to the sensing element of the force/torque sensor simultaneously. In the configuration of figure 7, the position of the sensing element in z direction and the angles θ_x and θ_y can be measured. By mounting the sensor in other two orthogonal orientations, the directions x, y and θ_z can be measured. In this way, the nonlinearities shown in figure 6 can be determined and compensated. Since the laser interferometer provides a traceable position and angle measurement, it is possible to calibrate the position and angle measuring system of the force/torque sensor and verify its stability as well. This step is fundamental in order to achieve the necessary positioning uncertainty. Figure 8 shows measurement results for the calibration in z direction. In this measurement,

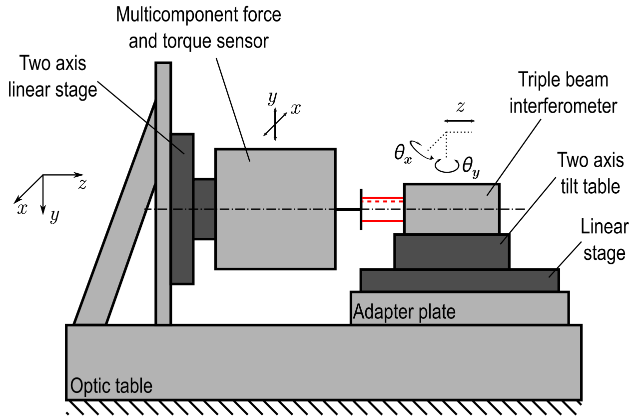

Figure 7. Calibration setup for position sensors.

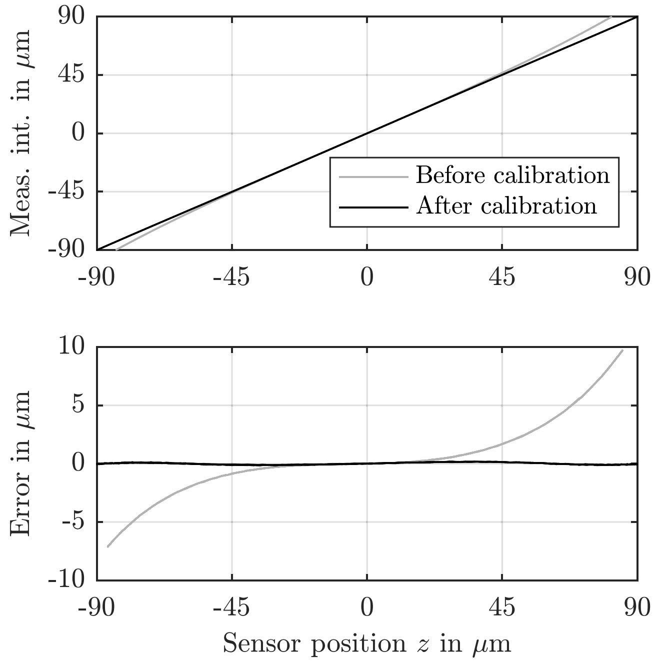

Figure 8. Measurement of the position in z direction before and after the calibration. The measurement result obtained with the laser interferometer is shown in the top plot. For the bottom plot, the error between measurements with laser interferometer and internal position measuring system is shown. The x axes contain measurement results from the internal position measuring system.

the position of the mirror was measured with the laser interferometer before and after the calibration. The measurement before the calibration was used to identify the nonlinearities. By using a polynomial approximation of third order, these nonlinearities were compensated and the measurement was repeated. In figure 8, the reduction of the effects caused by the nonlinearities can be observed. This procedure is used not only to compensated the nonlinearities in the internal position measuring system of the sensor, but also to eliminate the crosstalk between the position coordinates and angles.

2.3. Voltage, time and resistance measurement

The voltage, time and resistance traceable measurements are additional requirements for performing the self-calibration and measuring forces and torques with the required uncertainty. During the velocity mode, the amplitude of the voltage induced in the voice coil actuators must be determined with an uncertainty lower than 1 μV. The amplitude of the linear velocity v and the angular velocity Ω are obtained by measuring the amplitude of the position x or angle θ and multiplying it by the angular frequency of the movement ω:

$$v = x\omega, \quad \Omega = \theta\omega. \tag{8}$$

These expressions are only valid for a sinusoidal movement of the sensing element. That means the relative uncertainty of the velocity measurement is determined by the relative uncertainties of the position and frequency measurements. For this work, an angular frequency of $10 \cdot 2\pi$ rad s^{-1} is expected to be measured with a relative standard uncertainty smaller than $10 \cdot 10^{-6}$.

During the force/torque sensing mode the current i flowing in each voice coil actuator is determined by measuring the voltage drop u over a reference resistor R with a nominal resistance value of 10 Ω:

$$i = \frac{u}{R}. \tag{9}$$

The voltage drop must be measured with a standard uncertainty of 20 μV and the resistance must be known with a maximum relative standard uncertainty of $10 \cdot 10^{-6}$. The voltages are measured by using successive approximation analog-to-digital converter converters (ADC).

In order to assure the traceability for the time, resistance and voltage measurements, these components have to be calibrated. For the time measurement, this is done by comparing clock signals generated by the internal oscillator of the digital real-time controller (figure 2) with clock signals generated by a GPS disciplined oscillator, which provides a traceable time reference. The resistors are calibrated by measuring and comparing their resistance values with reference resistors, which are originally calibrated by using quantum Hall effect standards. The calibration of the voltage measuring system is performed with a voltage calibration device, which generates reference voltage levels. This device is originally calibrated by using a Josephson voltage standard.

2.4. Further considerations

Additional aspects of the system should be considered in order to achieve the desired measurement uncertainty for the force and torque measurements. This includes the thermal expansion of the sensor components, the presence of external magnetic fields, cross talk between the voice coil actuators, the presence of thermal electromotive forces (emfs) in electrical contacts, the level of local ground vibrations and the definition of a reference frame for the sensor. Most components of the sensor are made of aluminum and effects caused by thermal expansion can change the distance between the aperture slits and the respective dual photodiodes. The experimental setup of figure 7 can be used to analyze how these influences affect the measurement uncertainty for the position and angle measurements. External magnetic fields and magnetic fields of the coils overlap with the magnetic fields produced by the internal permanent magnets and influence the calibration factors k_{Bl} and k_{dBl}. Influences from static magnetic fields can be eliminated by executing a self-calibration task and determining new calibration coefficients, which consider the external fields. During the velocity mode, the voice coils B are used to move the sensing element while the voltages induced in the coils A due to the movement are measured. The alternating currents flowing in the coils B generate induced voltages in the coils A as well and cause an error in the measurement of the calibration factors. Therefore, the inductive coupling between the coils must be considered. For changing between the velocity mode and the force/torque sensing mode a switching system must be used. In order to avoid effects from thermal emfs in the electrical contacts, this switching system must be designed in a way to minimize temperature gradients. To provide isolation against ground vibrations, test measurements are performed on a table equipped with a vibration isolation system. Another important aspect for multicomponent force and torque measurement is the orientation of the reference frame of the sensor [32]. The sensor must provide a reference frame defined by some geometrical characteristics. This is necessary for properly aligning the sensor before executing a force measurement task.

3. Measurement uncertainty

The relative expanded uncertainty for the force and torque measurements can be estimated by considering a simplified model with only one voice coil actuator. For the force measurement, the following equation can be obtained from (1), (8) and (9) assuming that the calibration factor k_{Bl} is equal to the ratio obtained during the velocity mode u_{Bl}/v:

$$F = k_{Bl} i = \frac{u_{Bl}}{x\omega}\frac{u}{R}. \tag{10}$$

For the torque measurement, the following equation can be obtained from (2), (8) and (9) also assuming that the calibration factor k_{dBl} is equal to the ratio obtained during the velocity mode u_{dBl}/Ω:

$$T = k_{dBl} i = \frac{u_{dBl}}{\theta\omega}\frac{u}{R}. \tag{11}$$

Expressions for the combined measurement uncertainties of F and T can be obtained by using the method described in the guide to the expression of uncertainty in measurement [33]:

$$\frac{\sigma_F^2}{F^2} = \frac{\sigma_{u_{Bl}}^2}{u_{Bl}^2} + \frac{\sigma_u^2}{u^2} + \frac{\sigma_x^2}{x^2} + \frac{\sigma_\omega^2}{\omega^2} + \frac{\sigma_R^2}{R^2} \tag{12}$$

$$\frac{\sigma_T^2}{T^2} = \frac{\sigma_{u_{dBl}}^2}{u_{dBl}^2} + \frac{\sigma_u^2}{u^2} + \frac{\sigma_\theta^2}{\theta^2} + \frac{\sigma_\omega^2}{\omega^2} + \frac{\sigma_R^2}{R^2}. \tag{13}$$

For this uncertainty estimation, the cross-correlation between the variables was neglected as performed in [34]. Table 1 contains the single uncertainty contributions and the combined uncertainties for the force and torque measurements.

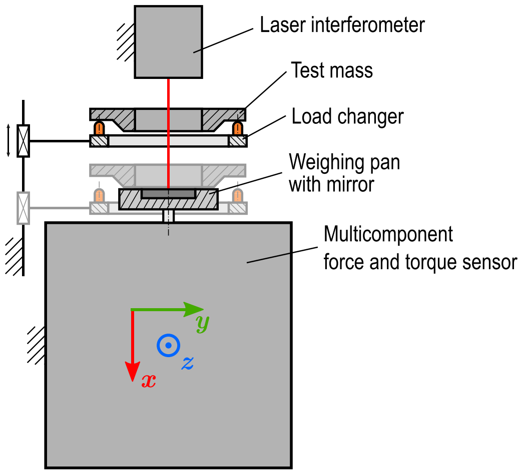

Figure 9. Measuring setup with multicomponent force/torque sensor, load changer and laser interferometer.

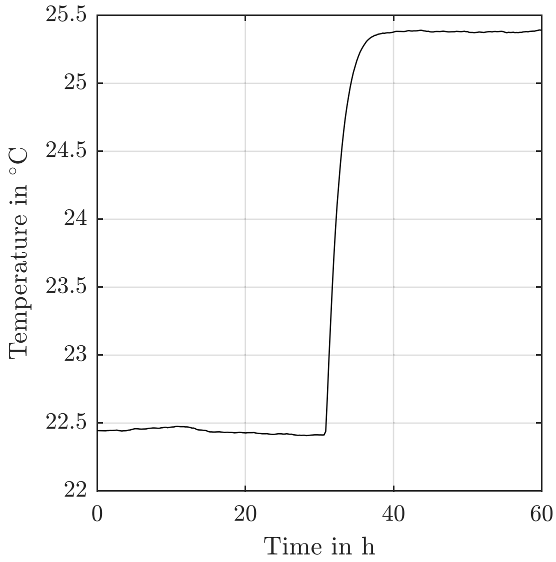

Figure 10. Temperature measured inside the sensor.

A maximal relative expanded uncertainty ($k = 2$) of $1 \cdot 10^{-4}$ is expected for the force and torque measurements in all components.

4. Measurement results

Preliminary measurements were performed with a prototype of the sensor to evaluate the type A uncertainties for the force measurement. Figure 9 shows the measuring setup used to obtain the results. It is composed by the self-calibrating multicomponent force and torque sensor, a load changer with a reference weight of 35 g and a laser interferometer. The laser interferometer was used for a preliminary evaluation of the stability of the aperture slit position sensors. This measuring setup is inside a climate chamber with controlled temperature, and a table with pneumatic vibration isolation system was used to avoid effects of ground vibrations.

In this experiment, the gravitational force generated by the test mass was measured using the self-calibrating

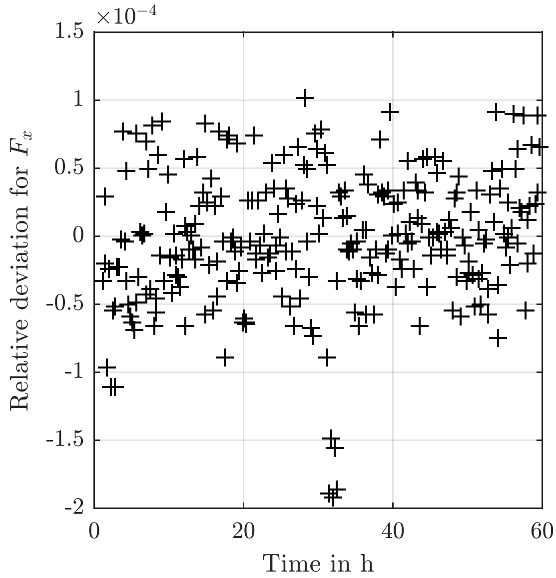

Figure 11. Relative deviation between the gravitational force generated by the test mass and the force F_x measured with the sensor.

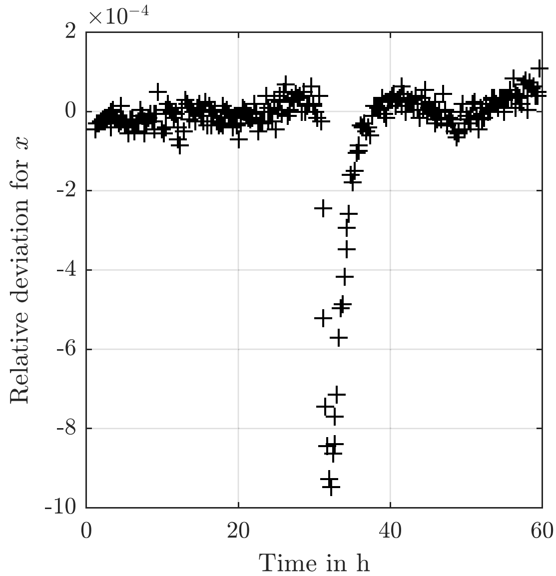

Figure 12. Deviation between the position measurement with the aperture slits and the laser interferometer in the x direction.

multicomponent force and torque sensor. For every measurement, a self-calibrating routine was executed and the weight force of the test mass was determined. For the velocity mode, the system was moved with sine wave trajectory with an amplitude of about 32 μm and frequency 10 Hz. The temperature was measured inside the sensor and, in order to obtain the results shown here, a temperature compensation was applied. The measurements were repeated for 60 h with a time interval of about 10 min between each measurement. Figure 10 shows the temperature measured inside the sensor. For the first half of the measurements, the ambient temperature was controlled at 20 °C and, for the second half, 23 °C. The temperature inside the sensor is about 2.4 °C higher than the ambient temperature. Figure 11 shows the relative deviation between the weight force generated by the test weight, which is about

Table 2. Measurement uncertainty contributions and combined measurement uncertainties.

Variable	Description	Value	Uncertainty σ	Relative Uncertainty
u_{Bl}, u_{dBl}	Induced voltage amplitude	37 mV	1 μV	$27 \cdot 10^{-6}$
u	Voltage drop in R	1 V	20 μV	$20 \cdot 10^{-6}$
x	Translation amplitude	30 μm	1 nm	$34 \cdot 10^{-6}$
θ	Rotation amplitude	580 μrad	20 nrad	$34 \cdot 10^{-6}$
ω	Movement frequency	$10 \cdot 2\pi$ rad s^{-1}	$100 \cdot 2\pi\,\mu$rad s^{-1}	$10 \cdot 10^{-6}$
R	Measurement resistor	10 Ω	100 $\mu\Omega$	$10 \cdot 10^{-6}$
F	Force measurement	2 N	98 μN	$49 \cdot 10^{-6}$
T	Torque measurement	0.1 N·m	5.0 μN·m	$50 \cdot 10^{-6}$

343 mN, and the force measured by the sensor in the x direction. In this figure, the bias of the measurements was canceled and only type A uncertainties are shown. For this measurement, a standard deviation of $43 \cdot 10^{-6}$ was obtained. This value is not considering the first 5 measurements performed after the temperature change. Figure 12 shows the relative deviation between the position measurement with the laser interferometer and the aperture slit sensors. A standard deviation of $34 \cdot 10^{-6}$ was obtained for this measurements. This value is not considering the first 21 measurements performed after the temperature change. The measurement results shown here are very near to the requirements listed in the table 2. However, more detailed investigations considering the torque measurement and type B uncertainties are still necessary.

5. Conclusion

The Kibble balance principle is being applied to the design of multicomponent force and torque sensors with the objective to improve and simplify the measurement of forces and torques. With the system proposed here it is not necessary to derive the force and torque quantities from the mass and gravity acceleration measurements. Instead, the forces and torques are derived from the measurement of voltages, positions, angles, resistances and time. In this way, the multicomponent force and torque sensor can be calibrated in conditions where the local gravity acceleration $\vec{g}$ is unknown or inexistent, as well as for any orientation relative to the $\vec{g}$ direction. The system is also an alternative to the traditional calibration methods for force and torque sensors, which use deadweights. Preliminary measurement results show that the required repeatability for the force measurement can be achieved. Future work will evaluate the repeatability for the torque measurement and the uncertainty for the multicomponent force and torque measurement.

Acknowledgments

The authors gratefully acknowledge the support by the Deutsche Forschungsgemeinschaft (DFG) in the framework of the Research Training Group Lorentz force velocimetry and Lorentz force eddy current testing (GRK 1567) at the Technische Universiät Ilmenau, Germany. This paper is an extended version of the work published in [35].

ORCID iDs

Rafael R Marangoni https://orcid.org/0000-0002-3546-5436
Jan Schleichert https://orcid.org/0000-0002-3679-686X
Thomas Fröhlich https://orcid.org/0000-0002-6060-7248

References

[1] Nitsche J, Baumgarten S, Petz M, Röske D, Kumme R and Tutsch R 2017 Measurement uncertainty evaluation of a hexapod-structured calibration device for multi-component force and moment sensors *Metrologia* **54** 171

[2] Baumgarten S, Kahmann H and Röske D 2016 Metrological characterization of a 2 kN · m torque standard machine for superposition with axial forces up to 1 MN *Metrologia* **53** 1165

[3] Ferrero C, Zhong L Q, Marinari C and Martino E 1993 New automatic multicomponent calibration system with crossed-exure levers *Proc. 3rd Int. Symp. on Measurement and Control in Robotics*

[4] Kim G S 2000 The development of a six-component force/moment sensor testing machine and evaluation of its uncertainty *Meas. Sci. Technol.* **11** 1377

[5] Parker P A, Morton M, Draper N and Line W 2001 A singlevector force calibration method featuring the modern design of experiments *Proc. 39th AIAA Aerospace Sciences Meeting & Exhibit*

[6] Rhew R D, Parker P A, Johnson T H and Landman D 2014 Variable acceleration force calibration system (VACS) *Proc. 9th Int. Symp. on Strain-Gaged Balance*

[7] Schleichert J 2015 Entwicklung und Untersuchung von Mehrkomponentensensoren für Kraft und Drehmoment *PhD Thesis* Technische Universität Ilmenau

[8] Parker P A and Liu T 2002 Uncertainty analysis of the single-vector force balance calibration system *Proc. 22nd AIAA Aerodynamic Measurement Technology and Ground Testing Conf.*

[9] Robinson I A and Schlamminger S 2016 The watt or Kibble balance: a technique for implementing the new SI definition of the unit of mass *Metrologia* **53** A46

[10] Haddad D, Seifert F, Chao L S, Li S, Newell D B, Pratt J R, Williams C and Schlamminger S 2016 Invited Article: A precise instrument to determine the Planck constant, and the future kilogram *Rev. Sci. Instrum.* **87** 061301

[11] Haddad D, Seifert F, Chao L S, Possolo A, Newell D B, Pratt J R, Williams C J and Schlamminger S 2017 Measurement of the Planck constant at the National Institute of Standards and Technology from 2015 to 2017 *Metrologia* **54** 633

[12] Davis R S 2015 What is a kilogram in the revised international system of units (SI)? *J. Chem. Edu.* **92** 1604–9
[13] Fröhlich T, Rahneberg I, Hilbrunner F and Schleichert J 2017 Vorrichtung und Verfahren zur Kalibrierung von Kraft- und Drehmomentmesseinrichtungen *German Patent* DE102016010668B3
[14] Gast T 1943 Eine registrierende Torsionswaage mit elektrischer Kompensation *German Patent* DE000000914445B
[15] Gast T 1955 Elektronische Waage *German Patent* DE000001035371B
[16] Hilbrunner F, Weis H and Fröhlich T 2014 Parameterization and optimisation of EMC balances based on the frequency response of the impedance *Measurement* **51** 349–55
[17] Schleichert J, Rahneberg I, Hilbrunner F and Fröhlich T 2016 Mehrkomponenten-Kraft- und -Drehmomentsensor nach dem Prinzip der elektromagnetischen Kompensation *Tech. Mess.* **83** 445
[18] Thess A, Votyakov E V and Kolesnikov Y 2006 Lorentz force velocimetry *Phys. Rev. Lett.* **96** 164501
[19] Hernández D, Marangoni R R, Schleichert J, Karcher C, Fröhlich T and Wondrak T 2018 Numerical and experimental study on vorticity measurement in liquid metal using local Lorentz force velocimetry *Meas. Sci. Technol.* **29** 035301
[20] Marangoni R R, Schleichert J, Rahneberg I, Mastylo R, Manske E and Fröhlich T 2017 Multi-component force measurement in micromachining *Tech. Mess.* **84** 587
[21] Will C, Behn C and Steigenberger J 2018 Object contour scanning using elastically supported technical vibrissae *ZAMM—J. Appl. Math. Mech.* **98** 289–305
[22] Birdwell J A, Solomon J H, Thajchayapong M, Taylor M A, Cheely M, Towal R B, Conradt J and Hartmann M J Z 2007 Biomechanical models for radial distance determination by the rat vibrissal system *J. Neurophysiol.* **98** 2439–55
[23] Shimachi S, Kameyama F, Hakozaki Y and Fujiwara Y 2005 Contact force measurement of instruments for forcefeedback on a surgical robot: acceleration force cancellations based on acceleration sensor readings *Medical Image Computing and Computer-Assisted Intervention* (Berlin: Springer) pp 97–104
[24] Berg D R, Kinney T P, Li P Y and Erdman A G 2011 Determination of surgical robot tool force requirements through tissue manipulation and suture force measurement *J. Med. Dev.* **5** 027517
[25] Sutton C M 2009 An oscillatory dynamic mode for a watt balance *Metrologia* **46** 467
[26] Hilbrunner F, Rahneberg I and Fröhlich T 2017 Wattwaage mit Hebelúbersetzung auf Basis eines kommerziellen EMK-Wägesystems *Tech. Mess.* (https://doi.org/10.1515/teme-2017-0065)
[27] Ahmedov H, Babayigit N, Korutlu B and Orhan R 2018 Preliminary Planck constant measurements via UME oscillating—magnet Kibble balance *Metrologia* **55** 326
[28] Li S, Schlamminger S, Haddad D, Seifert F, Chao L and Pratt J R 2016 Coil motion effects in watt balances: a theoretical check *Metrologia* **53** 817
[29] Schleichert J, Carlstedt M, Marangoni R R, Rahneberg I, Hilbrunner F and Fröhlich T 2016 Dynamische charakterisierung eines dreikomponenten kraftsensors mit Hilfe eines lorentzkraft-lastwechslers *Tech. Mess.* **83** 430
[30] Pyrhonen J, Jokinen T and Hrabovcova V 2009 *Design of Rotating Electrical Machines* 1st edn (New York: Wiley)
[31] Diethold C, Fröhlich T, Hilbrunner F and Jäger G 2010 High precission optical position sensor for electromagnetic force compensated balances *Proc. IMEKO 21st TC3 Int. Conf.*
[32] Nitsche J, Röske D and Tutsch R 2017 Influence of coordinate system alignment on the calibration of multicomponent force and moment sensors *Proc. IMEKO 23rd TC3 Int. Conf.*
[33] Working Group 1 of the Joint Committee for Guides in Metrology 2008 Evaluation of measurement data—guide to the expression of uncertainty in measurement
[34] Schlamminger S 2013 Design of the permanent-magnet system for NIST-4 *IEEE Trans. Instrum. Meas.* **62** 1524–30
[35] Marangoni R R, Schleichert J, Rahneberg I, Hilbrunner F and Fröhlich T 2017 A self-calibrating multicomponent force/torque measuring system *Proc. 59th Ilmenau Scientific Colloquium*